Colloid Polym Sci 273:708–716 (1995)

ORIGINAL CONTRIBUTION

W. Mächtle
G. Ley
J. Rieger

Ion exchange in carboxylated latices – AUC studies using sedimentation and density gradient techniques

Received: 8 July 1994
Accepted: 6 February 1995

Dr. W. Mächtle (✉) · G. Ley · J. Rieger
BASF Aktiengesellschaft
Kunststofflaboratorium
67056 Ludwigshafen, Germany

Abstract Crosslinked highly carboxylated acrylic latices with narrow particle size distributions were prepared by emulsion polymerization and characterized carefully by different AUC techniques (particle size distributions and particle density measurements). The acid form of those latices was neutralized with metal oxides like MgO, CaO, ZnO, or PbO in order to obtain the corresponding salt form of the latices which again were characterized carefully. The kinetics of the ion exchange between latex particles were studied by mixing, for example, the acid and the salt form of the latices monitoring the density distribution of the latex particles by density gradient ultracentrifugation. With all latices the hydrogen-metal ion exchange tends to be a complete one provided this process is given a sufficiently long exchange time. Theoretical models are provided which yield a qualitative explanation of the experimental data.

Key words Analytical ultracentrifuge – particle size distribution – density gradient – particle density distribution – carboxylated acrylic latices – ion exchange – metal oxides

Introduction

Crosslinking polymer latices by metal salts during film formation is known to result in excellent coatings [1]. Beside its economic impact, the ion exchange in carboxylated latices is an interesting field also with respect to fundamental research, because such latex particles actually representing submicron ion exchange beads are handsome models for studying analogous processes in regular polyelectrolytes.

In order to investigate the physical properties of metal salt crosslinked latices as well as the kinetics of the ion exchange taking place with the crosslinking process, a number of butyl acrylate-methacrylic acid copolymer "model" dispersions with different amounts of methylmethacrylate were prepared and then treated with metal oxides as MgO, CaO, ZnO, and PbO. Moreover, we wanted to demonstrate that the rarely employed ultracentrifuge density gradient technique is an excellent tool to study rather complex colloid systems and reactions.

Experimental

Samples

Two groups of latices, "softer" and "harder" ones, were prepared by emulsion polymerization. Latices having glass transition temperatures (T_g) below room temperature are called "softer", those having T_g's above room temperature are called "harder". The original "soft" latex, designed as mother-latex, consisted (by % wt.) of 78 *n*-butyl acrylate (*n*-BA), 20 methacrylic acid (MAA), and 2 methallyl methacrylate (MAMA), a crosslinking component. With respect

to the MAA-groups samples of this mother-latex were treated with stoichiometric amounts of solid MgO, CaO, ZnO, or PbO respectively, by stirring the mixtures at 85° centigrade for 3 h. The latices thus obtained were designated as "daughter-latices". All daughter-latices were carefully characterized by particle size distribution and particle density AUC measurements (see the next section).

A series of latices with increasing T_g was made up from (78-p) n-BA, 20 MAA, 2 MAMA, and p methyl methacrylate (MMA), with $p = 0, 10, \ldots 60$. These "harder" mother-latices were treated with stoichiometric amounts of ZnO only as described above. The resulting daughter-latices were carefully characterized, too. In order to study the kinetics of the ion exchange process, each daughter-latex was mixed with its corresponding mother-latex at a 1:1 mass ratio, the latices keeping their original polymer concentration of 10% by wt.

Measurements

All particle density and particle size distribution measurements were carried out by means of an analytical ultracentrifuge (AUC) the details of which have been described elsewhere [2–4]. By using a mixture of H_2O and the high density sugar metrizamide ($\rho = 2.1$ g/ml) as a dispergent instead of pure H_2O, the regular sedimentation run (S-run) is turned into a density gradient run (DG-run) [5]. Because in a DG-run particles gather in zones corresponding to their respective density thus causing narrow turbidity bands, the positions of which are stable once equilibrium has been reached (usually within 16 h); this method allows to determine particle densities very precisely. If the Schlieren optics used in S- and DG-runs is replaced by a turbidity optics, the light intensity I is measured as a function of time t during an AUC-run. From the $I(t)$-fractionation-curves obtained by this method the particle-size distributions (PSD) of the latices were calculated by means of Stokes' law and Mie's light scattering theory [2]. All AUC measurements are done at 25° centigrade.

Results and discussion

"Softer" latices

Figure 1 shows the integral (solid line) and the differential (broken line) PSD of the "soft" mother latex (78 n-BA/20 MAA/2 MAMA). The distribution is unimodal and narrow with latex particle diameters ranging between 200 and 300 nm. The inserted density gradient Schlieren photo shows a single narrow band. That means: All latex particles have exactly the same density, $\rho = 1.108$ g/ml, and, therefore, the same copolymer composition and the same equivalent percentage of H^+-ions. By treating this latex as described above with the metal oxides listed on the right-hand side of Fig. 1, the methacrylic acid will be transformed into the corresponding salts and the process will result in metallized daughter latices.

Our aim was to replace all light acid H-groups by the heavier metal ions having increasing atomic masses A_{Me}. The question is if it is possible to achieve a complete exchange, i.e., if not only the H-groups at the particle surface will be replaced, but also those deep inside the particle. A sketch of this complex situation is given in Fig. 2. Two neighboring H-groups are to be replaced by one double charged metal ion which in turn forms an ionic crosslink. Assuming the diameter of each particle does not

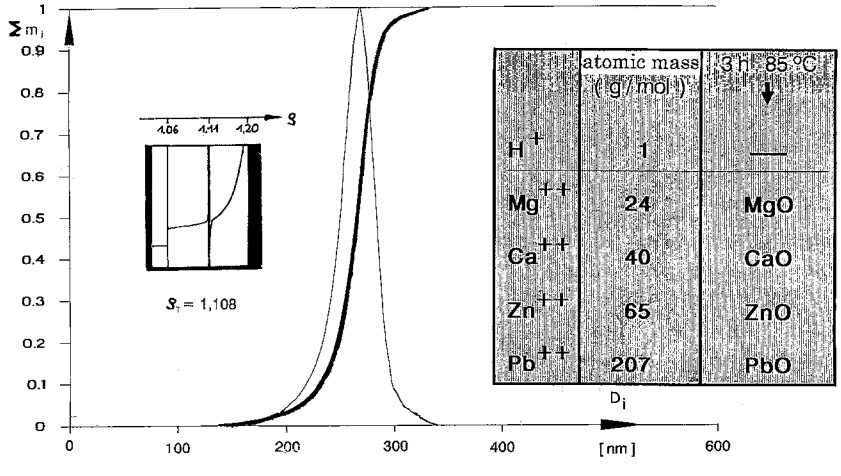

Fig. 1 Integral (———) and differential (-----) particle size distribution of the "soft" ($T_g = 11°$ C) mother-latex 78 n-BA/20 MAA/2 MAMA. Inserts: density gradient Schlieren photo (left); metal oxides with which the latex was treated and atomic masses of metal ions (right)

Colloid & Polymer Science, Vol. 273, No. 7 (1995)

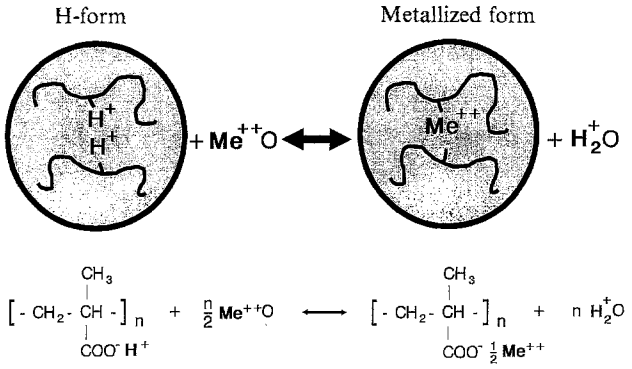

Fig. 2 Schematic diagram of molecular situation within a latex particle during Metal salt cross linking by $H^+ \leftrightarrow Me^{++}$ ion exchange

change when it is transformed from the acid into the metallized form, i.e., the volumes of a mother- and a daughter-particle are the same, a simple calculation of the particle density increase $\Delta\rho$ compared to the mother latex, resulting from a complete ion exchange, yields 0.019, 0.031, 0.047, and 0.099 g/ml (at 25 °C). In this calculation, for PMAA the latex particle density value $\rho_{PMAA} = 1.481$ g/ml and for metallized PMAA-Me the latex particle density value $\rho_{PMAA\text{-}Me} = [M(C_4H_6O_2Me_{0.5})/M(C_4H_7O_2)] \cdot \rho_{PMAA} = [(86 + 0.5\, A_{Me}])/87] \cdot \rho_{PMAA}$ was used, respectively. $\Delta\rho$ should be a linear function of the metal ion atomic mass A_{Me}.

Figure 3 shows the PSD's of the "soft" mother latex and of its daughter latices. Within experimental error limits, the distributions are all the same. Obviously, neither the colloidal state was disturbed by the metallization, nor did any agglomeration take place. The results of our DG-measurements on these latices are summarized in the schematic diagram of Fig. 4. All daughter latices show narrow bands (like the mother latex does), the bands taking positions corresponding to increased particle densities. That means, all particles of each kind have exactly the same metal content. The values of $\Delta\rho$ listed on the right-hand side of Fig. 3 are rather close to those obtained from the rough estimation mentioned above. From the insert on the left-hand side it is to be seen that $\Delta\rho$ is indeed a linear function of A_{Me}. As a surprising result it comes out that with each daughter latex all particles are *completely* loaded with the respective metal ions. That means, a complete hydrogen-metal ion exchange must have taken place, not only at the particle surfaces but also inside the particles.

"Harder" latices

Turning to the "harder" latices, the question is now whether a complete hydrogen-metal ion exchange will also take place in those latices consisting of $(78 - p)n$-BA/20 MAA/2 MAMA/p MMA. Figure 5 shows the PSD curves of the seven "harder" mother latices, the MMA content p of which having been varied stepwise from 0 to 60% by wt. All latices have narrow, unimodal, and nearly identical PSD's. The results of the DG-measurements on these latices are summarized in the schematic diagram in the center of Fig. 6. The monomer composition of the respective latex is listed on the left-hand side, the corresponding T_g is specified on the right-hand side of Fig. 6. All latices show narrow bands; that means they all are chemically homogeneous. The particle densities increase linearly

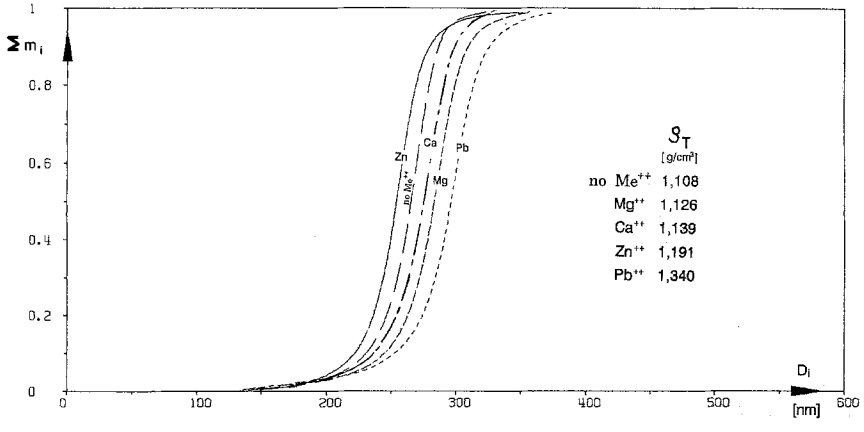

Fig. 3 Integral particle size distribution of the "soft" mother-latex 78 *n*-BA/20 MAA/2 MAMA and its four metallized daughter-latices

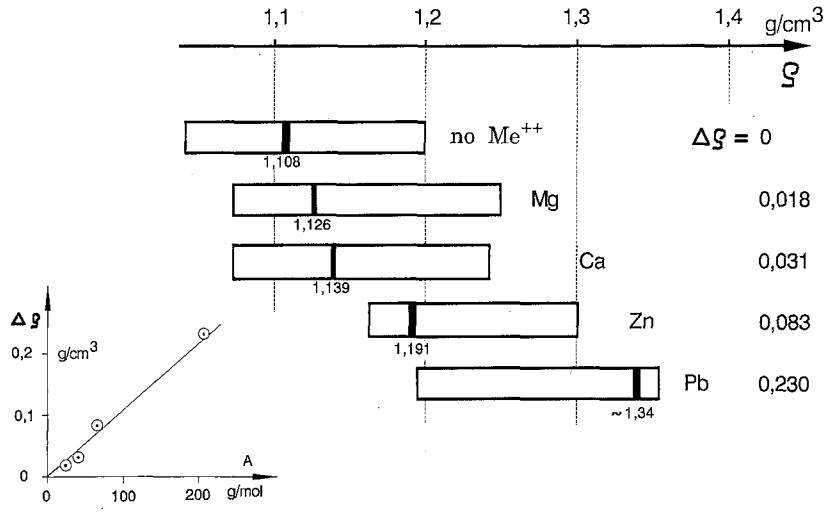

Fig. 4 Schematic diagram of the density gradient results on the "soft" mother-latex 78 *n*-BA/20 MAA/2 MAMA and its four metallized daughter latices. Inserts: Density increase $\Delta\rho$ by metallization vs. atomic mass of metal ions (left); amounts of $\Delta\rho$ (right)

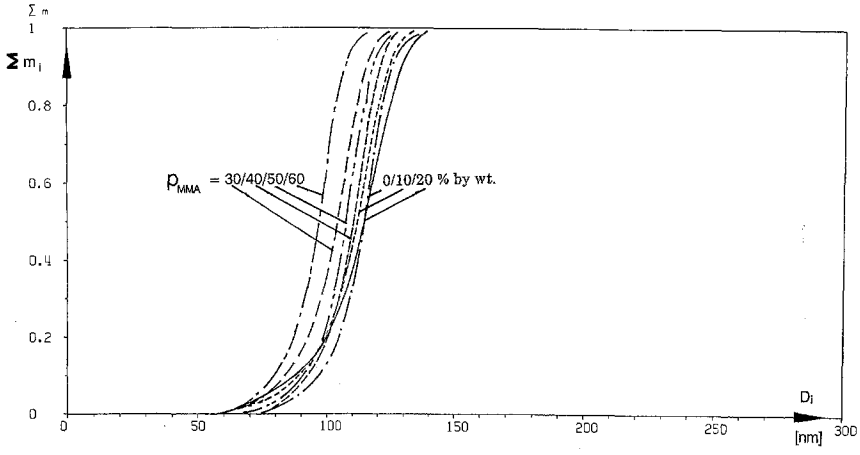

Fig. 5 Integral particle size distributions of the seven "harder" mother-latices (78 – *p*) *n*-BA/20 MAA/2 MAMA/*p* MMA); $0 \leqq p \leqq 60$

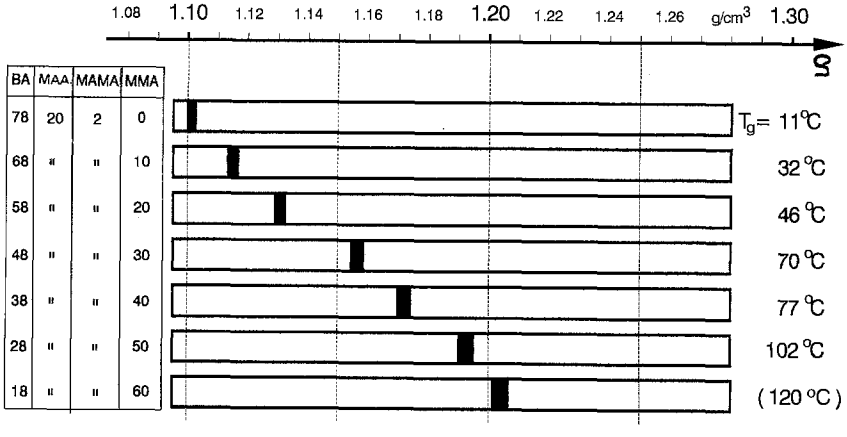

Fig. 6 Schematic diagram of the density gradient results on the seven "harder" mother-latices (78 – *p*) *n*-BA/20 MAA/2 MAMA/*p* MMA); $0 \leqq p \leqq 60$. Inserts: corresponding molecular compositions (left); glass transition temperatures (right)

with increasing MMA content. The latter in turn results in stepwise increasing "hardness" as indicated by T_g.

By treating these seven "harder" mother-latices with ZnO under the conditions described above, seven daughter-latices were obtained. As the distance between the treating temperature and the respective T_g was different for each latex (the latices containing 50 resp. 60% MMA were treated even below the T_g of the dry polymer!), we expected that only a partial ion exchange would have taken place in the five latices having T_g's below 85° centigrade.

But what did really happen? Figure 7 shows the PSD of the daughter-latices. Like in the case of the "soft" latices, the daughter-latices have – within the experimental error limits – the same narrow, unimodal PSD's, they being identical to those of the mother-latices. In Fig. 8 the results of the DG-measurements on the daughter-latices (filled bars) together with those of the mother-latices (open bars) are plotted in a diagram similar to that of Fig. 6. As in the case of the "soft" latices, all daughter-latices show narrow bands (like the mother-latices did) and particle densities increased by $\Delta\rho$ compared to their mother-latices. The $\Delta\rho$-values, listed on the right-hand side of Fig. 8, are approximately equal for all pairs of mother-daughter-latices, the mean value being $\Delta\rho = 0.077$ g/ml. That means, all daughter-latices are completely loaded with Zn^{++}-ions, even the two "hardest" ones. Thus, contrary to our expectations, in all cases a complete hydrogen-metal ion exchange took place, like in the "softer" latices.

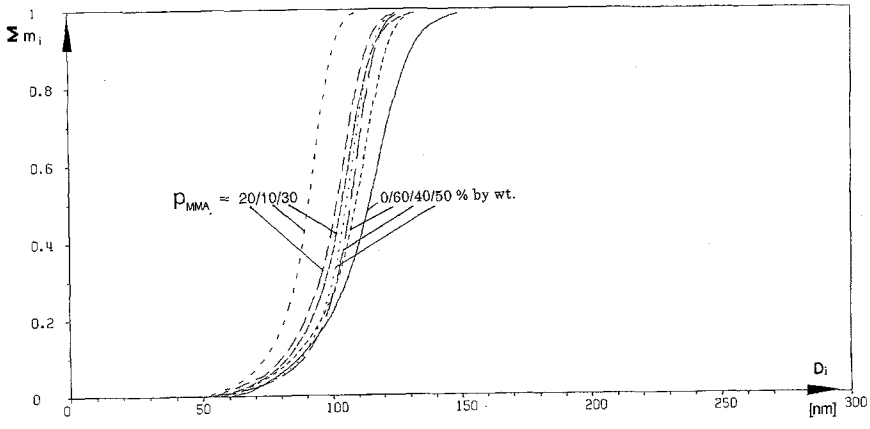

Fig. 7 Integral particle size distributions of the 7 (78 – p) n-BA/20 MAA/2 MAMA/ p MMA) metallized daughter-latices; $0 \leqq p \leqq 60$

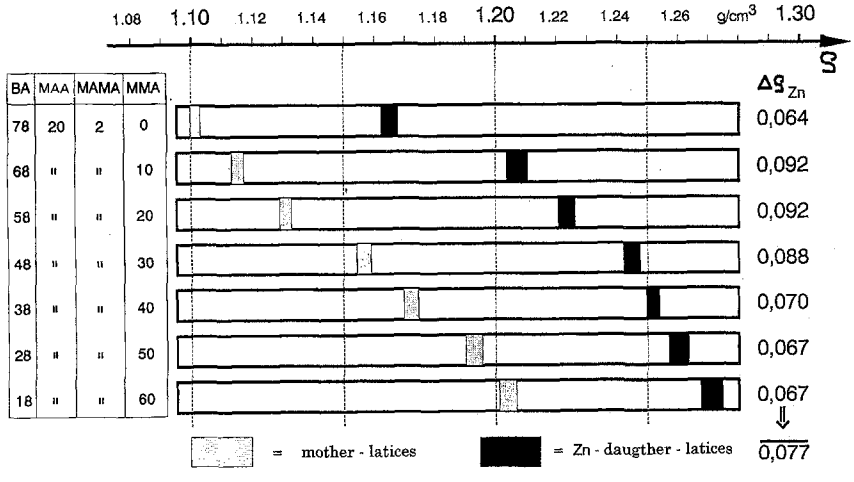

Fig. 8 Summarizing schematic diagram of the density gradient results on the 7 (78 – p) n-BA/ 20 MAA/2 MAMA/p MMA) mother-latices (open bars) and their metallized daughter-latices (filled bars). Inserts: corresponding molecular compositions (left); amounts of density increase $\Delta\rho$ by metallization (right)

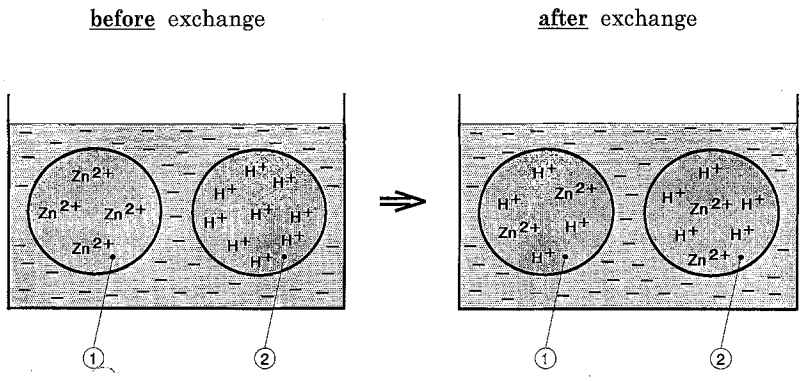

Fig. 9 Schematic diagram of latex particles before (left) and after (right) a complete $2H^+$-Zn^{++}-ion exchange between a mother- and a daughter-latex

Kinetics of the $H^+ \leftrightarrow Zn^{++}$-ion exchange

We will now turn to the mixtures of mother-latices with their metallized daughter-latices. These mixtures were prepared at room temperature, i.e., below the T_g of all latex pairs with the exception of the first one. In Fig. 9, a sketch of the ion exchange process is to be seen. The plot on the left-hand side shows the situation before the exchange, the plot on the right-hand side that at the end of a complete exchange. By this process the two kinds of particles having two different densities are transformed into one single kind of particle having a uniform density at the mean value of the initial densities.

In order to study the kinetics of this process in detail, samples were drawn from the mixing vessel after different exchange times. The samples were diluted to a ratio of 1:100, and then analyzed in a DG-measurement. Figure 10 shows the original DG-Schlieren photos obtained after an exchange time of 1 h. In the photo of the "softest" pair containing 0% MMA, only one single band is to be seen, while the photos of all other mixtures exhibit two distinct, very narrow bands indicating two kinds of particles having different densities, i.e., different Zn contents. For the four samples containing between 30 and 60% MMA, these densities correspond approximately to those of the initial components of the respective mixture.

The situation after an exchange time of 3 days is schematically plotted in Fig. 11. Now also for the mixtures containing 10 and 20% MMA the initial bands of the mother-latex (open bars) and daughter-latex (hatched bars) have merged into one single band (full bars), respectively, in the mean position. That means, in these samples the $2H^+ \leftrightarrow Zn^{++}$-ion exchange is fully completed after 3 days. With the four remaining "harder" samples, the distance between the mixture bands has decreased compared to the situation of Fig. 10, and it will decrease more in relation to increasing exchange time.

In Fig. 12 are summarized all our DG-measurement results on these mixtures after exchange times of 1 h, 3 days, 9 days, 30 days, and 85 days. For each mixture the positions of the DG-Schlieren bands obtained are plotted

Fig. 10 Density gradient Schlieren photos of the 7 $(78-p)$ *n*-BA/20 MAA/2 MAMA/p MMA) mother/daughter-latex (1:1) mixtures after 1 h exchange time

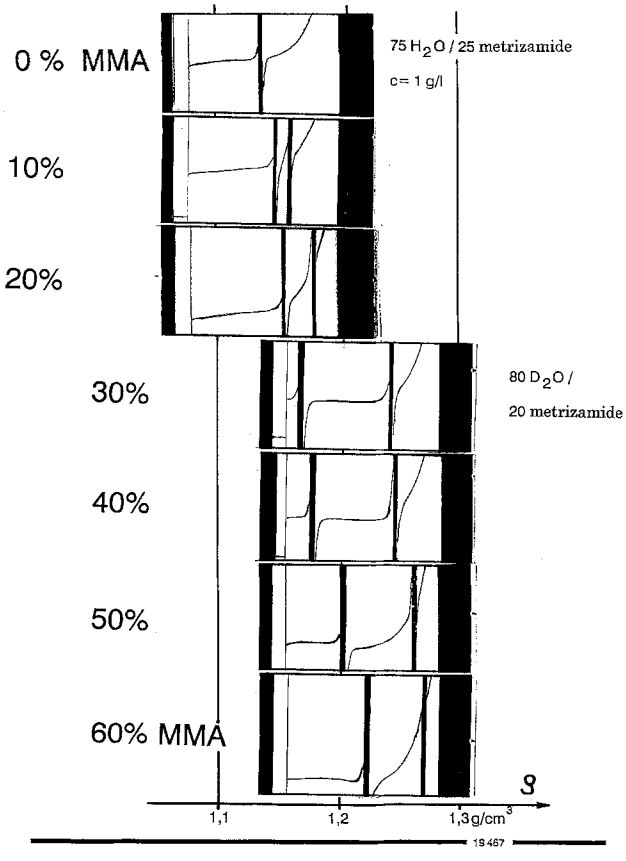

Colloid & Polymer Science, Vol. 273, No. 7 (1995)

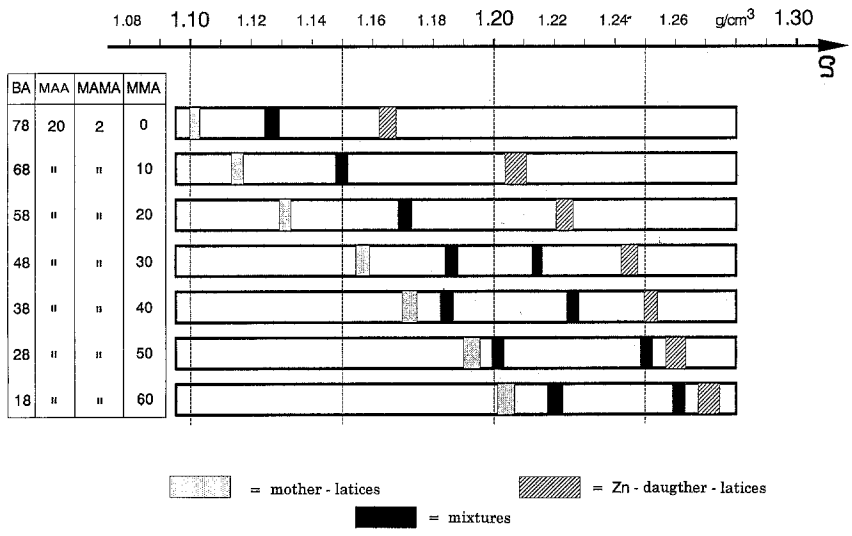

Fig. 11 Summarizing schematic diagram of the density gradient results on the (78 − *p*) *n*-BA/20 MAA/ 2 MAMA/*p* MMA) mother-latices (open bars), their daughter-latices (hatched bars), and respective (1:1) mixtures after 3 days exchange time

along the ρ-axis as a function of the exchange time indicated. It comes out clearly that in all seven mixtures a complete $2H^+ \leftrightarrow Zn^{++}$-ion exchange will take place even at room temperature if only the exchange process is given a sufficiently long time. The rate of this process depends on the MMA content, too: the higher the latter, the lower the exchange rate.

Fig. 12 Summarizing schematic diagram of the density gradient results on the (78 − *p*) *n*-BA/20 MAA/2 MAMA/*p* MMA) latices after different exchange times. For details see text

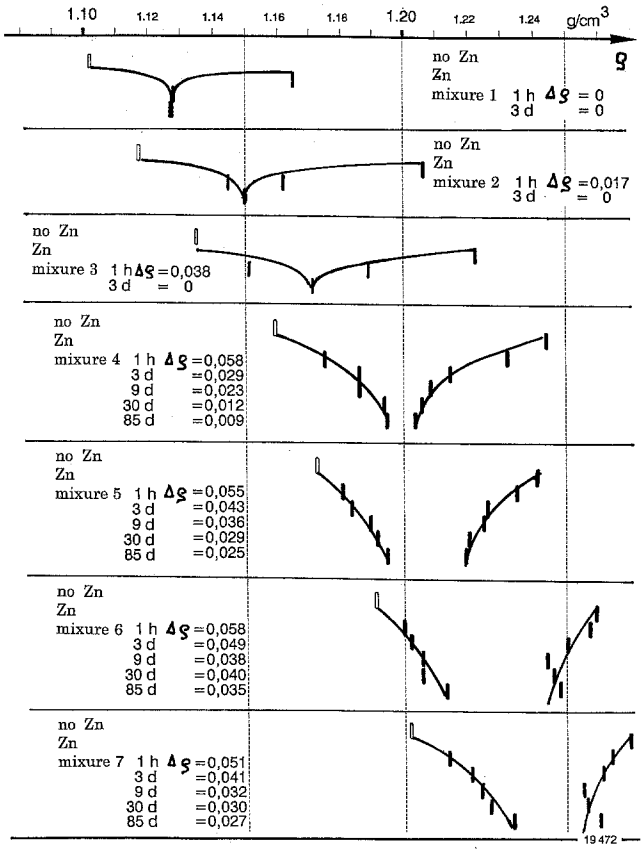

Models for the exchange of ions between latex spheres

Looking at the density gradient results, cf. Fig. 12, it seems at first sight quite surprising that the Schlieren bands are very narrow. Intuitively, one expects a successive broadening of the bands because of diffusion effects. In the following, we sketch two theoretical models for the microscopic processes of ion-exchange between the latex spheres. These models yield a qualitative explanation of the experimental results. A detailed discussion of the theoretical considerations will be given elsewhere.

For simplicity, we term the two types of ions black and white ions. It is assumed that their charge is + e and that their diffusion constants do not differ. A system of N latex spheres freely diffusing in an inert medium, each carrying M ions, is considered. In both models we start at $t = 0$ with $N/2$ latex particles carrying M white ions and $N/2$ particles carrying M black ions.

Model A: The latex spheres exchange ions upon collision

By collision, we mean the close approach of two latex particles during their diffusion in the serum. The main assumption of this model is that the type of ion exchange, viz. white-white, white-black, black-white, or black-black, depends on the respective number of black/white ions on the two latex spheres. In a first order approach the probability p_{ij} of exchanging an ion of type i against an ion of

type j ($i, j \in$ {black, white}) is given by $p_{ij} = f_{1i} f_{2j}$, where f_{1i}/f_{2j} is the fraction of ions of type i/j on particle 1 or 2 of the two colliding spheres. It is assumed that on the average a time interval τ_A elapses between two collision events in the system. τ_A is determined by the diffusion constant D of the latex spheres in the serum and by the volume fraction ϕ of latex particles, $\tau_A \propto R^4/(D\phi^2)$. R is the radius of the latex spheres. In each of the collision events two of the N latex spheres collide and exchange one pair of ions according to the above probability. This process is an extended version of the Bernoulli–Laplace model for diffusion and was treated by means of Monte Carlo simulations. The result of such a simulation is shown in Fig. 13, where we have chosen $N = 100$ and $M = 10^4$. Comparing Fig. 13 with the experimental results in Fig. 12, one notices that the results of model A indeed coincide with the experiment: two narrow bands approach each other. Analysis of the simulation data gives the following information. The shape of the bands can be described by a Gaussian with the relative variance given by $\sigma' = \sigma/M \propto M^{-1/2}$. The two bands approach each other according to a simple exponential time law, where the time constant is given by τ_A.

What is the reason for the narrowness of the bands? A first hint is the above relation for the variance of the bands which scales as $\sigma \propto M^{1/2}$. Remember that in simple Brownian diffusion, one has $\sigma \propto n^{1/2}$, where n is the number of random walk steps. Thus, we have a situation which looks as if it is related to some standard diffusion process. And, indeed, one can show for the case $N = 2$ *via* the appropriate difference equations and Fokker–Planck equations that our Model A is a realization of a diffusion process in a potential. The crucial point for understanding why the bands look so narrow is the following: in the present discussion we investigate the evolution of the system on a scale given by M, which corresponds to $\Delta\rho$ in the DG-experiment. On this scale, with M defining our observation window, σ seems to decrease as M increases. Or stated in a different way, the relative variance σ' decreases as M increases. This point becomes clear, when pursuing the analogy with classical diffusion: usually, diffusion processes or random walks are depicted on a scale set by $n^{1/2}$. Thus, the random walk fills the window of observation. Our approach of using n for setting the scale results in an effective shrinking of the diffusion path to a point as $n \to \infty$. We used the unconventional scale of M because in our model there is a one-to-one correlation to the $\Delta\rho$ scale of the DG-experiment.

Fig. 13 Computer simulation of the ion-exchange process between $N = 100$ diffusing latex spheres according to Model A, see text. The figure shows the time evolution of the fractions of latex particles carrying m black ions. Number of ions per sphere: 10^4

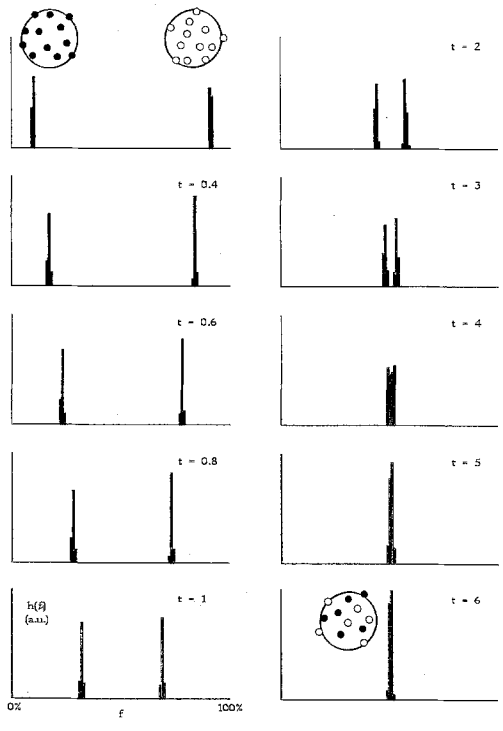

Computer-histogram: number h(f) of particles holding a portion of f_1 - particles on their surface.
For t = 0 (start of simulation) is:
h(0) = h(100) = N/2 , N = 100 , M = 10000.

Model B: Ion exchange via the liquid phase

On the average, each latex sphere carries αM ions ($\alpha < 1$). Those ions which are not bound to a particle diffuse in the serum. It is assumed that per time interval τ_B each latex particle exchanges one bound ion with one free ion. In our approach the concentration of black and white ions in the serum is equal. Thus, it suffices to investigate the ion-exchange statistics of a single latex particle. The probability p_{ij}, defined above, depends solely on the fraction of black and white ions on this particle: $p_{ij} = f_i$, where $f_i = n_i/(\alpha M)$ and n_i is the number of bound ions of type i ($i \in$ {black, white}). The difference equation describing the time evolution of Model B yields in the appropriate limit a Fokker–Planck equation which can be solved analytically. The results are similar to the ones obtained for Model A. Concerning the qualitative description of the experimental DG-data, this implies that Model B works as well as Model A. It must be stressed that the Donnan effect is taken into account in both models implicitly via the statistical mechanical approach used.

With the present knowledge it is not possible to discriminate between Models A and B. What one can learn

Colloid & Polymer Science, Vol. 273, No. 7 (1995)

from the above discussion is that our simple approach is sufficient to understand some of the experimental findings which look surprising at first sight. But, there is an important difference between the two models with regard to future investigations on the mechanism of ion-exchange between latices or, more generally, polyelectrolyte molecules. It can be shown that the relevant time scale in Model A is determined by $\tau_A \propto R^7/\phi^2$ if the ions are distributed over the surface of the latex sphere and $\tau_A \propto R^8/\phi^2$ if the ions are distributed over the volume of the sphere. For Model B one can estimate that $\tau_B \propto R^2/\phi^{2/3}$. By measuring the rate with which the bands in a DG-experiment approach each other as a function of R and ϕ it should be possible to decide which model is the more appropriate one. This information would be of great interest for the understanding of the behavior of polyelectrolytes.

Conclusion

It has been shown that the latex particles of normal polymer dispersions can be described as ion exchanger particles with colloidal dimensions. Our study on well characterized monodisperse "model" polymer dispersion systems shows that in carboxylated latices essentially all carboxylic groups, both at the surface and in the interior of the latex particle, can be neutralized using metal (hydr)oxides without interfering with the colloidal stability of the systems. The resulting well characterized metal ion loaded daughter latices can be used for studying the kinetics of the ion exchange process in mixtures with the corresponding mother latices which represent the H-form of the colloidal ion exchanger particles.

While the equilibrium distribution of the cations in the mixtures is independent of the copolymer composition, the kinetics of the ion exchange process show large matrix effects, despite the tiny size of the ion exchanger particles. We are able to understand and even to model some aspects of the exchange process, which at first sight seems to be very curious, e.g, the occurrence and preservation of discrete "populations" of exchanger particles with distinct metal content during the exchange process. This behavior stems from the high number of exchangeable ions per particle ($\sim 10^5$) coupled with either a stepwise exchange of the ions between the exchanger particles or a very low equilibrium concentration of the metal ions in the serum. Better measurements are needed to judge these alternatives.

Well characterized ion exchanging latex particles seem to be valuable model systems for studies on fundamental properties of polyelectrolytes.

References

1. Warson H (1972) The Applications of Synthetic Resin Emulsions. E Benn London pp 911 ff
2. Mächtle W (1984) Makromol Chem 185:1025–1039
3. Mächtle W (1984) Colloid Polym Sci 262:270–282
4. Mächtle W (1991) Progr Colloid Polym Sci 86:111–118
5. Meselson M, Stahl FW, Vinograd J (1957) Proc National Acad Sci 43:581